Food Chemistry: X 15 (2022) 100410

Contents lists available at ScienceDirect

Food Chemistry: X

journal homepage: www.sciencedirect.com/journal/food-chemistry-x

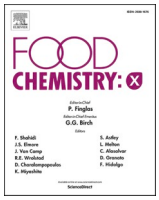

Preparation and characterization of low oil absorption corn starch by ultrasonic combined with freeze–thaw treatment

Shiyu Zhang [a,b], Qi Li [a,b], Yang Zhao [a,b], Zhixin Qin [a,b], Mingzhu Zheng [a,b,*], Huimin Liu [a,b], Jingsheng Liu [a,b,*]

[a] College of Food Science and Engineering, Jilin Agricultural University, Changchun, Jilin 130118, China
[b] National Engineering Research Center for Wheat and Corn Deep Processing, Changchun, Jilin 130118, China

ARTICLE INFO

Keywords:
Corn starch
Low oil absorption
Ultrasonic
Freeze–thaw
Long-range and short-range structure

ABSTRACT

This study investigated the effects of ultrasonic, freeze–thaw, and combined pretreatments on corn starch oil absorption. Low-field nuclear magnetic resonance (LF NMR) was used to study the oil absorption changes after frying of corn starch (CS) subjected to different treatments. The structural characteristics of samples were evaluated using various techniques. Scanning electron microscopy, contact angle, and particle size analysis showed that corn starch subjected to combined ultrasonic and freeze–thaw treatment generated larger, coarser particles with a denser structure. Furthermore, X-ray diffraction, Fourier transform infrared spectroscopy, and differential scanning calorimetry showed that combined treatment improved the order and thermal stability of CS molecules, thereby inhibiting oil absorption during frying. The results showed that combined ultrasonic and freeze–thaw pretreatment significantly reduced the oil absorption of corn starch before and after frying.

Introduction

Starch is a polymer carbohydrate mainly composed of amylose and amylopectin (Timm et al., 2020). Starch can be directly hydrolyzed by enzymes in the human body to provide energy. Therefore, starch is among the most important natural polymers in daily life. With the rapid development of the modern food industry, starch has become the main raw material for food processing. Frying is a cumbersome process, involving heat transfer and the interaction between food and oil. Owing to the complicated and fast frying process, various problems can emerge that seriously affect consumer health. A diet rich in high-oil foods can increase the risk of obesity, diabetes, and even cardiovascular and cerebrovascular diseases (Ching et al., 2021). Considerable research effort has focused on reducing the oil content of fried food. The approaches used can be divided into coating treatment (Aminlari, Ramezani, & Khalili, 2016; Hua, Wang, Yang, Kang, & Yang, 2015), frying pretreatment and post-treatment, and the reconfiguration of products (Debnath, Bhat, & Rastogi, 2003; Fauster et al., 2018; Zeng et al., 2016).

Previous studies have shown that pretreatment before frying is an effective strategy for reducing the oil content of starch-based fried foods. Presently, starch is mainly modified by crosslinking, chemical, and physical methods. Han, Lee, and Lim (2007) observed that the addition of crosslinked starch can inhibit oil absorption during frying. Chemical modification is quick and simple, but is not usually environmentally friendly, and can easily cause chemical residues in the product (Hu et al., 2013). Enzymatically modified starch is often used to prepare absorbent starch (Guo et al., 2021), which is difficult to apply to reduce oil absorption. Furthermore, enzymes are sensitive to temperature, pH, and ions, and controlling enzymatic modification is difficult, resulting in its rare use in food. Accordingly, physical modification remains the dominant strategy among current methods.

Ultrasonic treatment is a physical method used to modify starch. Soundwaves with a frequency higher than 20 kHz causes the collision of liquid particles, which creates pressure through cavitation, resulting in particle-to-particle interactions (Wang et al., 2020). As a nonthermal pretreatment, ultrasonic treatment is widely used in food processing and commercial applications. Studies have shown that ultrasonic treatment had a great influence on the granular structure of starch (Zhu, Li, Chen, & Li, 2012), particle size (Sujka, 2017), and swelling degree (Jambrak et al., 2010). Zhang et al. reported that low-power ultrasonication significantly reduced the oil content of potato chips (Zhang, Yu, Fan, & Sun, 2021b). Freeze–thaw treatment is another method for processing modified starch. For starch samples above 0 °C, water between particles penetrates through channels between surface gaps and pore sizes, while

* Corresponding authors at: College of Food Science and Engineering, Jilin Agricultural University, Changchun, Jilin 130118, China.
E-mail addresses: Zhengmzhu@163.com (M. Zheng), liujs1007@vip.sina.com (J. Liu).

https://doi.org/10.1016/j.fochx.2022.100410
Received 23 April 2022; Received in revised form 21 July 2022; Accepted 4 August 2022
Available online 8 August 2022

for samples below 0 °C, the internal water freezes, expands, and squeezes the starch particles. During this freeze–thaw process, the surface becomes rough and cracks can appear. Studies have shown that multiple freeze–thaw treatments affect the granular structure of starch and leaching of amylopectin, and hinder the increase in its relative crystallinity (Tao et al., 2015).

The physical modification of starch particles by freeze–thaw treatment has been extensively studied, but its effects on the oil absorption of starchy fried foods have rarely been investigated. As for the topic of ultrasonic treatment to reduce the oil content in fried foods, most studies used potato or whole flour as material. Other chemical compounds, such as proteins and lipids would affect the physicochemical properties of starch during the treatments. Although a single treatment has been successfully applied to starch modification, few reports have combined two or more treatments to prepare modified starch with improved functional properties. An efficient, fast, and low-cost method to reduce the oil content of fried food is extremely necessary. Therefore, the present study aimed to investigate the effect of combined ultrasonic and freeze–thaw pretreatment on the oil absorption of starch granules. Furthermore, the physicochemical characteristics and structure of normal corn starch (CS) affected by combined ultrasonic and freeze–thaw treatment were analyzed. With increasing attention being paid to food health, studying the influence of combined ultrasonic and freeze–thaw treatment on the performance of corn starch is important. This also provides a theoretical basis for the production of healthy low-fat starch-based fried foods in the food processing industry.

Materials and methods

Materials

Corn starch was provided by Yuanye Co. ltd. (Shanghai, China). Soybean oil was purchased at a Walmart supermarket (Changchun, China). All solutions were prepared with deionized water. All chemicals and reagents were of analytical grade.

Sample preparation

Ultrasonic treatment

Corn starch was dispersed in distilled water in a 1:9 (w/v) ratio and fully mixed with magnetic stirring for 10 min. Samples were prepared using a 1200-W ultrasonic breaker (Ningbo, China). The vibrating titanium tip probe (diameter, 13 mm) was immersed in the starch solution intermittently (repeated cycles of ultrasonication for 2 s and no ultrasonication for 2 s) for 20 min. During this process, the starch sample was immersed in a water bath at a constant temperature of 25 ± 0.5 °C. Ultrasonic power levels of 60, 120, 180, 240, and 300 W were used, with the corresponding samples denoted as U1–U5, respectively.

Freeze–thaw treatment

Starch samples were subjected to freeze–thaw treatment according to the method of Liu et al. (Liu et al., 2019), with a slight modification. Corn starch (10 g) and deionized water (15 mL) were mixed in a centrifuge tube at a temperature of 25 ± 0.5 °C, then frozen at − 20 °C for 22 h and thawed at 30 ± 0.5 °C for 2 h. This freeze–thaw cycle was conducted 1–5 times, with the corresponding samples denoted as FS1–FS5, respectively.

Combination treatment

In previous trials, the lowest oil absorption rate was obtained by treatment with an ultrasonic power of 60 W. Therefore, this ultrasonic treatment was combined with freeze–thaw treatment, as described above, for 1–5 cycles, with the corresponding samples denoted as U1-FS1, U1-FS2, U1-FS3, U1-FS4, and U1-FS5, respectively.

Simulated fried starch

Fried starch samples were prepared according to the method of Chen (Chen et al., 2018a), with a slight modification. The starch sample (1 g) and soybean oil (10 mL) were mixed thoroughly in a 100-mL beaker with magnetic stirring for 10 min, and then placed in an oil bath preheated at 180 °C for 20 min. Unbound oil was separated from the sample by vacuum filtration to obtain the final samples.

All samples were dried at 40 °C for 24 h, passed through a 100-mesh sieve, and stored in a sealed state for further study. Untreated corn starch was used as the control group.

Sample absorption

Total oil/water absorption of samples

The determination of starch oil/water absorption was based on the method of Yousif (Yousif, Gadallah, & Sorour, 2012), with a slight modification. The starch sample (1 g) was weighed into a 15-mL centrifuge tube, mixed with oil/water (10 mL), and shaken for 10 min. The mixture was then centrifuged at 4000 rpm for 20 min. The supernatant was discarded and inverted until oil no longer flowed out. The test tube and mixture were then weighed. The oil/water absorption was calculated using the following equation:

$$absorption\,\% = W - W_0/W_0 \times 100\%$$

where W_0 (g) is the weight of the starch sample before absorption and W (g) is the weight of the mixture after absorption.

LF NMR determination of total oil amount in fried samples

The total oil content of fried starch was measured using the method of Yang (Yang et al., 2020). A 23-MHz NMR analyzer (NMI20, Shanghai, China) was used for quantitative analysis of the reference substance (soybean oil) and samples. A sample of the certain quality was weighed into a glass bottle and sealed to avoid evaporation. The sample was transferred to an NMR tube, and the transverse spin relaxation (T_2) signal was collected by stimulation with the Carr-Purcell-Meiboom-Gill (CPMG) pulse sequence at a constant temperature of 32 °C.

The oil calibration curve was established by linear regression analysis between the corresponding peak area of the NMR signal and the oil mass in the tube. Pure soybean oil was used as the standard substance to quantitatively analyze oil in samples. The oil content of the fried sample was then calculated by measuring the NMR signal peak area and using a calibration curve. Signals of all samples were obtained under the same conditions.

Scanning electron microscopy (SEM)

The sample microstructure was observed using an electron microscope (Sigma 300, USA). Samples were evenly dispersed on conductive tape and vacuum sprayed with gold for 5 min. The acceleration voltage was set to 15 kV, and samples were observed at 1000 × and 5000 × magnification.

Particle size determination

The starch particle size was analyzed according to the method of Simkova (Šimková, Lachman, Hamouz, & Vokál, 2013). A particle size analyzer (BT-9300HT, Dandong, China) was used to determine the particle size distribution of starch granules. Distilled water was used as the dispersion medium and dry sampling was performed. The particle size distribution was measured by scanning for 30 s, with a measurement range of 0.1–716 μm.

Contact angle

The contact angle (θ) of samples was measured using a basic static and dynamic contact angle meter (SL200KS, Shanghai, China). The

starch samples were compressed into flakes and placed on a sample slide. A high-precision sampler was then used to slowly drop 2 μL of oil onto the sample slide, and images of the droplets were taken using a high-speed camera.

Fourier transform infrared (FT-IR) spectroscopy

FT-IR analysis of the starch samples was performed using a VERTEX 70 FTIR instrument (Bruker, Germany). Samples (2 mg) were mixed with KBr (0.2 g) and ground into a uniform powder in an agate mortar. The resulting powder was pressed into thin sheets and measured in the wavenumber range of 4000–400 cm^{-1} at 25 °C to obtain FT-IR spectra.

X-ray diffraction (XRD)

XRD analysis was performed according to the method of Qiao (Qiao et al., 2017), with a slight modification. The crystal structure of starch samples was determined using a D/MAX2500 X-ray diffractometer (Rigaku Corporation) with Cu Kα radiation of 40 kV and 30 mA. The scanning angle was in the range of 4–45°, and the scanning rate was 5°/min. The relative crystallinity (RC) of samples was calculated using the following equation:

$$relative\ crystilinity\% = IC/(IC + IA) \times 100\%$$

where IC and IA are the cumulative diffraction intensities of the crystalline and amorphous regions of the sample on the diffractogram, respectively.

Differential scanning calorimetry (DSC)

The thermal properties of samples were measured by DSC (Q2000, TA Company, USA). Starch samples (3 mg) and deionized water (9 μL) were mixed in an aluminum pot and equilibrated for 12 h at 4 °C. An empty aluminum pot was used as the control. The temperature was increased from 30 to 120 °C at a rate of 10 °C/min, and the nitrogen flow rate was 50 mL/min. The onset temperature (T_o), peak temperature (T_p), conclusion temperature (T_c), and gelatinization enthalpy (ΔH) of this process were recorded.

Statistical analysis

All results were means ± standard deviation of triplicate experiments. One-way analysis of variance (ANOVA) was performed for each sample using Tukey's test in SPSS 24.0 software.

Results and discussion

The adsorption capacity of starch

The oil absorption of different corn starch samples is shown in Fig. 1. The oil absorption rate of corn starch initially decreased and then increased. When starch samples were treated with different amounts of ultrasonic power, the oil absorption rate changed significantly ($p < 0.05$). The oil absorption rate of corn starch decreased from 81.33 % for CS to 75.33 % for U1 (Fig. 1A). Compared with the oil absorption rate of natural corn starch (CS), different freeze–thaw treatment cycles also significantly affected the oil absorption rate of starch ($p < 0.05$). For sample FS3 (three freeze–thaw cycles) the oil absorption rate decreased to 67.67 % (Fig. 1B). As U1 was determined to be the sample with the lowest oil absorption from ultrasonic treatment, the oil absorption rate of samples prepared by ultrasonic treatment at 60 W combined with different numbers of freeze–thaw cycles was measured, as shown in Fig. 1C. Starch subjected to combined ultrasonic and freeze–thaw treatment gave a minimum oil absorption rate of 61.67 % (U1-FS2). The oil absorption rates of U1, FS3, and U1-FS2 had decreased by 7.38 %, 16.80 %, and 24.17 %, respectively, compared with CS. The oil

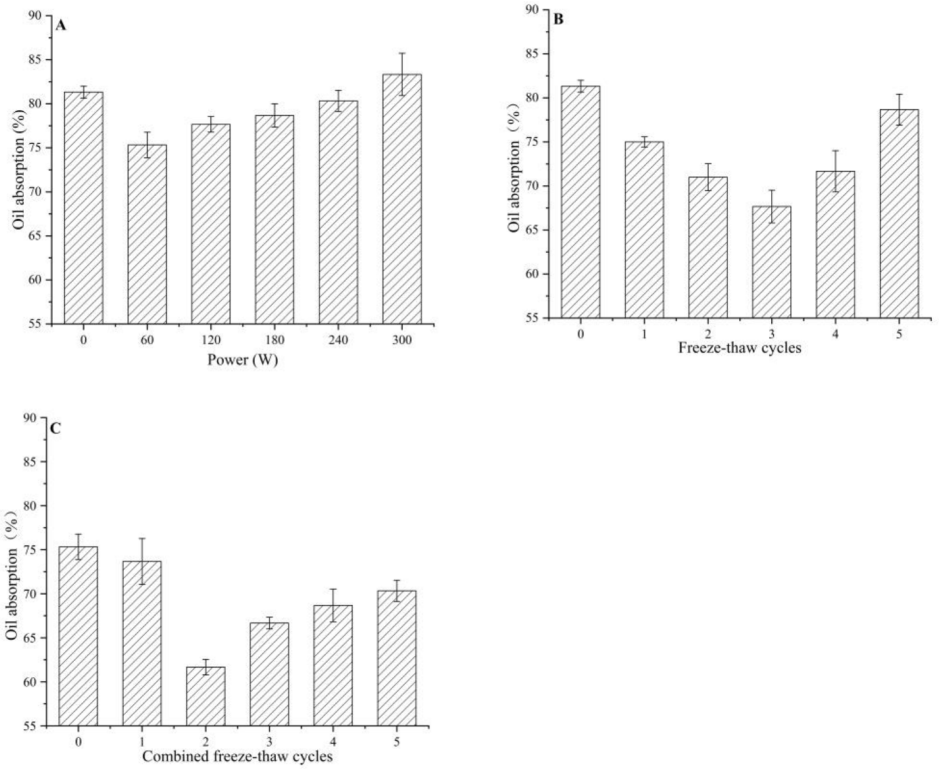

Fig. 1. The total oil absorption rate of starches with different treatments. A, The oil absorption rate of starches treated with different ultrasonic power; B, The oil absorption rate of starches treated by different freeze–thaw cycles; C, The oil absorption rate of starches treated by 60 W ultrasonic power combined with different freeze–thaw cycles.

absorption rate of corn starch decreased more significantly under the combined treatment ($p < 0.05$). This might be due to the combined treatment causing more damage to the starch granules than the single treatment. In the combined treatment, ultrasonic treatment provided channels in starch granules for the entry of water molecules during subsequent freezing and thawing treatment. Furthermore, corn starch subjected to ultrasonic treatment and only two freeze–thaw cycles gave the lowest oil absorption rate. The reasons for this required further investigation. Therefore, representative samples U1, FS3, and U1-FS2 were selected for analysis.

As shown in Table 1, the total water absorption of samples CS, U1, FS3, and U1-FS2 was measured. Compared with untreated CS, the water absorption rates of U1, FS3, and U1-FS2 were increased by 27.31 %, 33.52 %, and 35.19 %, respectively. Therefore, the water absorption rate of starch clearly increased after treatment, in contrast to the oil absorption rate. This showed that these treatments did not reduce the oil absorption and water absorption of the sample simultaneously.

Fried starch oil content

The standard curve for oil and the linear regression equation are shown in Fig. 2. The coefficient of determination (R^2) of the linear regression equation was higher than 0.999, confirming the high correlation between the relative peak area of the relaxation spectrum and the relative oil content.

The oil content of simulated fried starch is shown in Table 2. The oil content of fried corn starch was 36.74 % (CS). Ultrasonic starch (U1) had an increased oil content compared with CS, but the difference was not significant ($p > 0.05$), in contrast to the results of previous studies (Dehghannya, Naghavi, & Ghanbarzadeh, 2016). The oil content of U1-FS2 was reduced to 29.08 %, showing that combined ultrasonic and freeze–thaw treatment was a more effective method for preparing low-oil corn starch compared with single treatments. Frying involves complex heat transfer and mass transfer processes. During frying, oil slowly penetrates from the surface through to the interior. Therefore, the decreased oil content might be related to the starch structure.

Scanning electron microscopy

The SEM micrograph of starch samples is shown in Fig. 3. The untreated CS particles had an irregular polygonal structure with a smooth surface, which was similar to the conclusion of Diop (Diop, Li, Xie, & Shi, 2011). The surface of U1 was roughened and tiny holes had formed, which might be due to the cavitation effect of ultrasonic waves. It was observed that a rough surface could greatly improve the oleophobicity (Zhu, Li, Xing, & Gui, 2021). Ultrasonic treatment could roughen the surface of starch, resulting in the reduction of the total oil absorption. Individual U1 starch granules were damaged, and the broken starch granules caused the oil to overflow. Although there were small pores on the surface of starch granules under ultrasonic treatment, oil was removed from the pores with centrifugation. The surface of FS3 from freeze–thaw treatment was also very rough with a denser structure. Zhao et al. (Zhao, Law, & Sambhy, 2011) previously observed that increased surface roughness inhibited oil absorption. In the freeze–thaw process, water flowed into the sample interior through gaps between starch granules. When water formed ice crystals during freezing, pressure was exerted on nearby particles, which formed a dense structure that effectively reduced the contact area with oil. When the ice crystals melted into water during thawing, dents were formed on the particle surfaces. In the combined treatment, starch granules were first subjected to ultrasonic treatment to form surface cavities, which was conducive to the penetration of water molecules. After freeze–thaw treatment, more water molecules acted on the starch particles, which significantly affected the surface and structure of starch granules. This might be the main reason for sample U1-FS2 showing the lowest oil absorption rate. Notably, the dense starch structure made oil absorption more difficult. These starch granules with a dense structure showed some thermal stability and resisted destruction of the granular structure during frying. This might also be a key reason for the decreased oil content after the frying process.

Table 1
The water absorption and frying oil absorption of starches with different treatments.

Samples	Total water adsorption (%)	Fried starch oil content (%)
CS	64.67 ± 1.86a	36.56 ± 0.27c
U1	82.33 ± 1.20b	36.90 ± 0.60c
FS3	86.35 ± 1.45bc	32.50 ± 0.27b
U1-FS2	87.43 ± 0.67c	29.08 ± 0.33a

CS, corn starch; U1, 60 W ultrasonic power treatment starch; FS3, 3 cycles of freeze–thaw treatment starch; U1-FS2, 60 W ultrasonic treatment combined with 2 cycles of freeze–thaw treatment starch. Different letters in the same column indicate significant differences ($p < 0.05$).

Contact angle of starch samples

The contact angle, which defines the wetness of liquid spreading on the solid surface, is an important intuitive parameter for analyzing the surface absorption of starch (Vadgama & Harris, 2007). Therefore, the size of the contact angle directly reflects the interaction between the oil phase and starch sample. The contact angles between oil droplets and the starch surface are shown in Fig. 4. All angles were$<90°$, which indicated that starch had natural lipophilicity. The contact angle of the untreated starch was 21.96°, while those of modified starches had increased to 24.45° (U1), 25.74° (FS3), and 28.45° (U1-FS2). Zhu et al. (Zhu et al., 2021) reported that the increased roughness might not be conducive to the spreading of oil droplets. This might be due to the surface roughness of the sample being relatively large after combined treatment, which inhibited oil spreading on the starch surface. This was consistent with SEM results above. The increased contact angle proved that the lipophilicity of treated starch was reduced. The contact angle of U1-FS2 was largest, which was consistent with the total oil absorption results.

Particle size analysis

The particle size distribution diagram of the samples showed that all samples contained large, medium, and small starch granules (Fig. 5). Compared with CS, the content of medium and small particles had increased in sample U1 after ultrasonic treatment, while the change in the content of large particles was not significant. This might be attributed to low-power ultrasonication having a greater impact on medium and small starch particles, which could be decomposed into relatively small particles. However, the small and medium particle contents of FS3 and U1-FS2 were significantly decreased, while their large particle contents had increased considerably. This was probably due to liquid water forming solid ice during the freezing processes, causing the sample particles to swell and increase in volume. Compared with single ultrasonic and freeze–thaw treatments, the combined treatment afforded more large particles. Ultrasonic pretreatment not only increased the number of small particles in the starch, but also ruptured the surface of particles, thereby increasing the penetration of water molecules. Therefore, more small molecular particles absorbed water and swelled into large molecules during freeze–thaw cycling, which was the main reason for the increased particle size. Compared with large particles, the small starch particles showed a larger surface area and more readily absorbed water and swelled. Furthermore, the small particles had smaller voids, which increased the oil holding capacity. The swelling property of small starch particles was also stronger (Vamadevan & Bertoft, 2015). The more open structures of these expanded starch granules were expected to make them more conducive to oil absorption

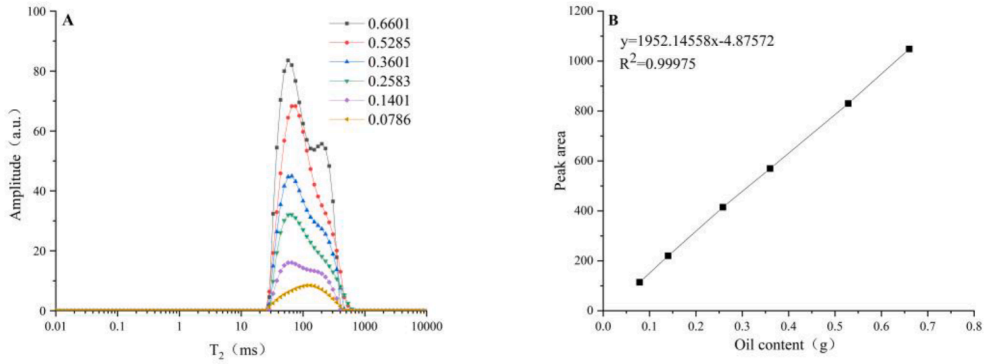

Fig. 2. A is the transverse relaxation spectrum of oil CPMG proton; B is the standard curve of oil quantitative analysis.

Table 2
Analysis of particle size of starches with different treatments.

Samples	D_{10}(μm)	D_{50}(μm)	D_{90}(μm)	$D_{4,3}$(μm)	Specific surface area (m^2 /kg)
CS	1.98 ± 0.40b	12.80 ± 0.19b	27.54 ± 0.46b	20.99 ± 0.11a	276.10 ± 0.06bc
U1	1.78 ± 0.25a	11.62 ± 0.33a	26.42 ± 0.83a	20.34 ± 0.49a	279.23 ± 0.28c
FS3	2.49 ± 0.50c	14.08 ± 0.25c	108.04 ± 0.26c	32.56 ± 0.41b	258.00 ± 0.95b
U1-FS2	3.38 ± 0.17d	14.69 ± 0.17d	128.17 ± 0.19d	40.95 ± 0.11c	237.63 ± 0.97a

CS, corn starch; U1, 60 W ultrasonic power treatment starch; FS3, 3 cycles of freeze–thaw treatment starch; U1-FS2, 60 W ultrasonic treatment combined with 2 cycles of freeze–thaw treatment starch. Different letters in the same column indicate significant differences ($p < 0.05$).

during frying. Therefore, the starch granules subjected to combined treatment (U1-FS2) had a larger content of large particles and showed the lowest oil content (Table 1).

The particle size and specific surface area of samples are shown in Table 2. Different treatments had significant effects on the particle size and specific surface area of samples ($p < 0.05$). $D_{4,3}$ represents the average particle size. With a limited moisture content, the state of particles after frying remained unchanged. Therefore, the particle size played a leading role in the oil absorption process, which explained why the smallest particles had the highest oil absorption rate. The specific surface area represents the total area per unit mass of an object. Although the specific surface area of sample U1 after ultrasonic treatment was increased compared with that of CS, the difference was not significant ($p > 0.05$). It showed that starch granules were looser after ultrasonic treatment. The frying process is accompanied by complex heat and mass transfer reactions, and the loose structure may increase the penetration of grease during frying. When measuring the starch adsorption capacity, the surface roughness of starch is one of the main reasons for inhibiting its absorption of oil. Therefore, the oil absorption of ultrasonic treated starch before and after frying had different trends. The specific surface areas of freeze–thaw treated starch (FS3) and combined-treatment starch (U1-FS2) were significantly reduced. The contact area between the sample and oil was also proven to be reduced, resulting in reduced oil absorption by starch. Generally, a rougher surface on starch granules results in a larger surface area. However, the increase in particle size had a more significant impact on the surface area.

FT-IR spectra of starch samples

FT-IR spectroscopy is a method used to quickly determine the short-range ordered structure of starch, which is sensitive to changes in starch. The FT-IR spectra of corn starch and modified starch are shown in Fig. 6. The functional groups had not changed, with no new functional groups generated. However, the absorption peak of modified starch had changed compared with that of the original starch. Absorption peaks in the range of 1200–800 cm^{-1} were due to C—C and C—O vibrations (Jeroen, Soest, Tournois, Wit, & Vliegenthart, 1995). Furthermore, the ratio of absorption peak heights at 1047 and 1022 cm^{-1} ($R_{1047/1022}$) represented the relative contents of short-range ordered structures in starch (Sevenou, Hill, Farhat, & Mitchell, 2002). The $R_{1047/1022}$ value of increased from 1.256 for CS to 1.278 for U1, indicating that the short-range order of starch molecules increased after ultrasonic treatment. This might be attributed to the recrystallization of short chains increasing the ordered structure (Zhang et al., 2021a), or low-power ultrasonication mainly affecting the amorphous area, but having little effect on the crystalline area (Bonto, Tiozon, Sreenivasulu, & Camacho, 2021). For these reasons, the $R_{1047/1022}$ value had increased. The $R_{1047/1022}$ value of FS3 after freeze–thaw treatment had decreased to 1.253. During the freeze–thaw treatment, water molecules generated ice crystals in the crystalline and amorphous areas, resulting in severe damage to both areas, which reduced the order of starch molecules. After combined treatment, the $R_{1047/1022}$ value of U1-FS2 had increased to 1.299. The results showed that combined ultrasonic and freeze–thaw treatment helped to improve the short-range ordered structure of starch.

The intensity of the absorption peak at 995 cm^{-1} represented the number of hydrogen bonds in molecules. Therefore, the height ratio of the absorption peaks at 1022 and 995 cm^{-1} ($R_{1022/995}$) represented the interaction between starch and water molecules (Chen et al., 2021). The $R_{1022/995}$ values of U1 (0.998), FS3 (1.014), and U1-FS2 (1.030) were increased compared with that of CS (0.986). Therefore, treatments had enhanced the interaction between starch and water molecules, which was consistent with our previous water absorption results for starch.

The peak at 2928 cm^{-1} corresponded to the stretching vibration of polysaccharide methylene groups (CH_2), which is related to the lipophilicity of starch (Santha, Sudha, Vijayakumari, Nayar, & Moorthy, 1990). U1, FS3, and U1-FS2 showed reduced absorption peak intensities for polysaccharide methylene groups compared with CS, proving that the starch lipophilicity was reduced, which explained the decrease in starch oil absorption.

XRD analysis of starch samples

XRD was used to analyze changes in the long-range ordered structure of starch. As shown in Fig. 6, both the original and modified starches showed single peaks at around 15° and 23°, and adjacent shoulder peaks at 17° and 18°, which were characteristic of A-type crystals (Ye, Liu, Luo, Hu, & McClements, 2018). Therefore, ultrasonic and freeze–thaw

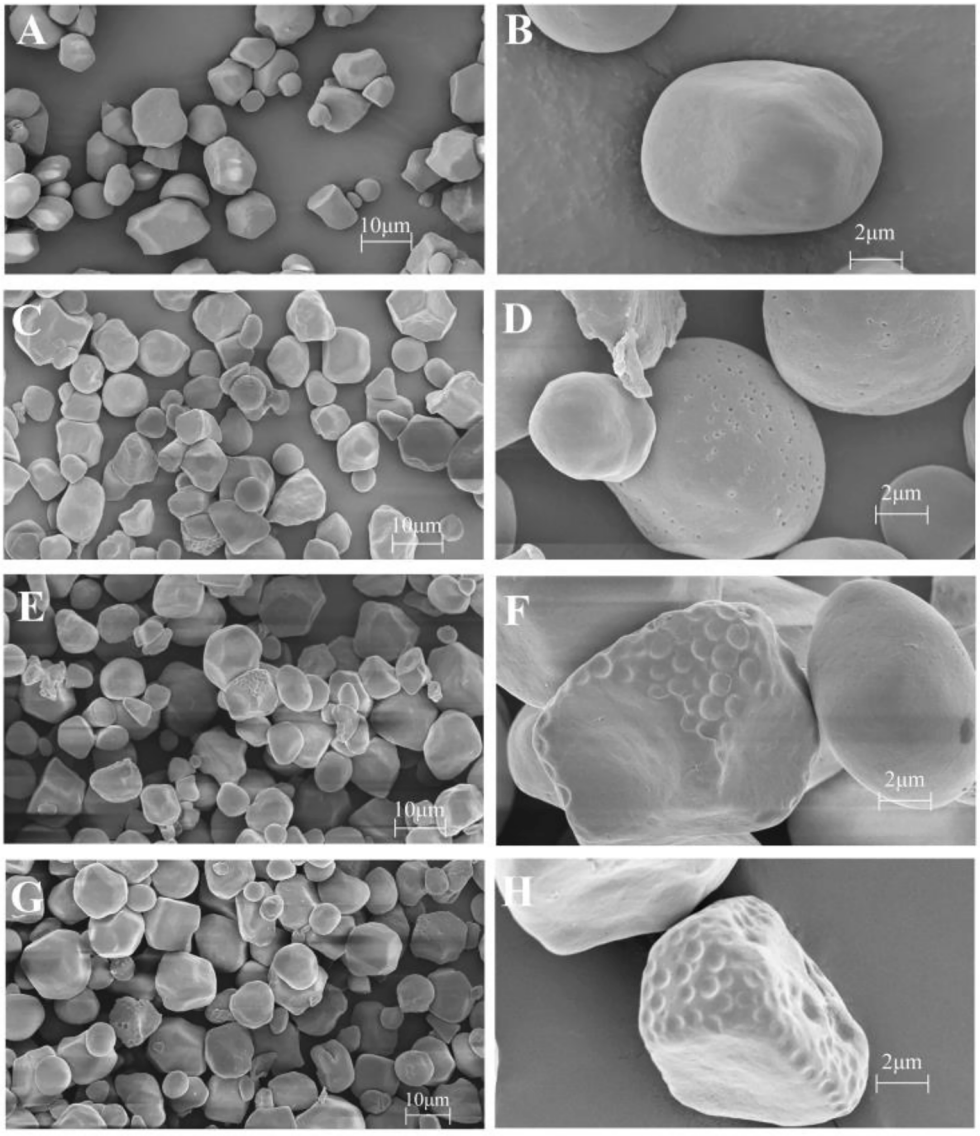

Fig. 3. SEM images of starches with different treatments. A and B, CS, corn starch; C and D, U1, 60 W ultrasonic power treatment starch; E and F, FS3, Freeze-thaw treatment starch; G and H, U1-FS2, 60 W ultrasonic treatment combined with 2 cycles of freeze–thaw treatment starch.

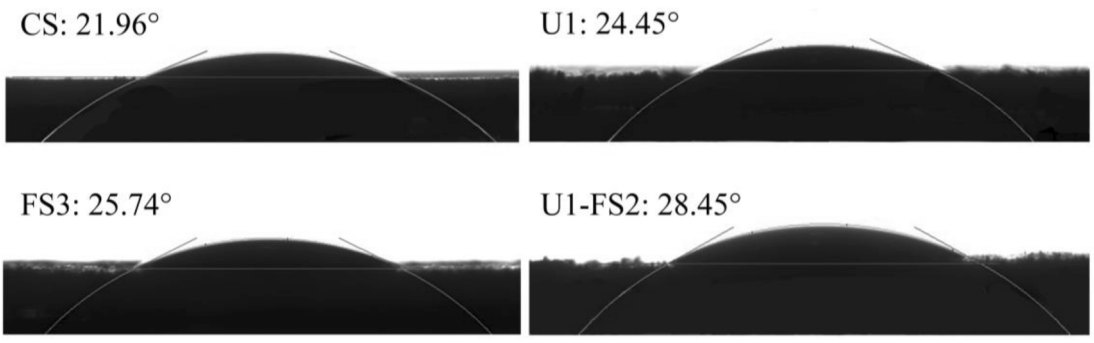

Fig. 4. The contact angles with oil of starches with different treatments.

treatment methods did not change the crystal form of the starch, with the A-type structure maintained after treatment. However, the crystallinity of starch had changed. The relative crystallinity (RC) values of modified U1, FS3, and U1-FS2 were 26.08 %, 25.45 %, and 21.39 %, respectively, which were lower than that of CS (30.11 %). The decrease in crystallinity was mainly related to destruction of the crystal structure (Liu, Wang, Liao, & Shen, 2020). This showed that both ultrasonic and freeze–thaw treatments affected the starch crystallization area. The

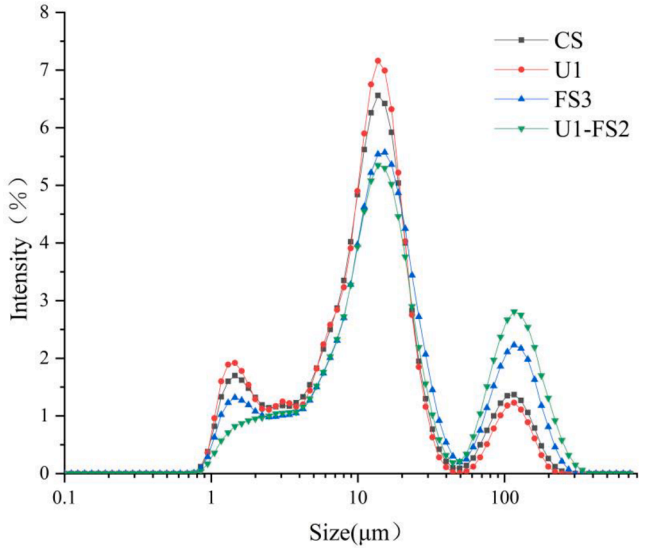

Fig. 5. The particle size distribution diagram of starches with different treatments.

decreased RC of U1 was attributed to low-power ultrasonic treatment mainly affecting the amorphous area (Bonto et al., 2021). The short-term decreased was also limited. The RC of FS3 after freeze–thaw treatment had decreased. This might be due to water entering the starch granules and forming ice crystals during the freezing cycle. The granules swelled with the formation of ice crystals, causing hydrogen bonds between molecules to break and crystal alignment to be lost (Liu et al., 2019). Compared with the results of single ultrasonic and freeze–thaw treatments, U1-FS2 from combined treatment showed the smallest RC value, which was related to ultrasonic pretreatment leading to more water molecules entering the starch granules, resulting in further destruction of the crystalline area.

A faint characteristic peak was observed at 20°, which represented the V-type complex (Chanvrier et al., 2007). Starch is mainly composed of amylose and amylopectin, in which amylose and lipid molecules easily form V-type complexes (Chen et al., 2018). Compared with CS, the peak intensity of the sample after treatment at 20° showed no obvious change (Fig. 6), which indicated that ultrasonic and freeze–thaw treatments had little effect on the complexation between amylose and lipid molecules in the sample.

Thermal characteristics of starch samples

To verify the effect of ultrasonic and freeze–thaw treatments on the thermal properties of corn starch, DSC measurements were performed on samples CS, U1, FS3, and U1-FS2. The results are shown in Table 3, which summarizes the DSC parameters of samples subjected to different treatments. Starch swells and splits at high temperatures to form a paste solution, in a process known as starch gelatinization. The onset temperature (T_o) represents the degree of starch gelatinization. Compared with single physical treatment methods, the T_o of U1-FS2 after combined treatment was significantly increased, indicating that the gelatinization process was delayed. U1-FS2 required a higher temperature to gelatinize, which might reduce the oil absorption by U1-FS2 during simulated frying, resulting in a reduced oil content during frying (Table 1). This was related to dissolution of the weak crystal structure in starch granules, which might make the structure of starch molecules more ordered (Tao, Wang, Wu, Jin, & Xu, 2016). The gelatinization enthalpy (ΔH) reflects the energy required to dissociate the double helix structure in the starch crystal region (Luo et al., 2021). The decrease in ΔH indicated that less energy was needed to destroy the double helix structure, proving that double helix structures in the starch crystallization zone were lost after ultrasonic and freeze–thaw treatments. This result was in agreement with the results of XRD (Fig. 6). The DSC results again confirmed that ultrasound combined with freeze–thaw treatment reduced the breakdown of the starch structure during frying, thus inhibiting the penetration of oil.

Conclusions

This study investigated the effects of ultrasonic, freeze–thaw, and combined treatments on normal corn starch (CS) oil absorption and structural changes. Combined ultrasonic and freeze–thaw treatment significantly reduced oil absorption by corn starch. The results of SEM, CA, particle size analysis, XRD, FT-IR, and DSC showed that combined

Table 3
Analysis of thermal properties of starches with different treatments.

Samples	T_o(°C)	T_p(°C)	T_c(°C)	ΔH (J/g)
CS	65.34 ± 0.26a	68.32 ± 0.45a	75.33 ± 0.26ab	10.13 ± 0.19c
U1	65.78 ± 0.16a	69.24 ± 0.33a	74.58 ± 0.17a	8.98 ± 0.23b
FS3	66.00 ± 0.26a	68.79 ± 0.38a	75.00 ± 0.32a	8.72 ± 0.20b
U1-FS2	67.34 ± 0.27b	71.45 ± 0.29b	76.15 ± 0.23b	8.05 ± 0.11a

T_o, onset temperature; T_p, peak temperature; T_c, conclusion temperature; ΔH, gelatinization enthalpy. Different letters in the same column indicate significant differences ($p < 0.05$).

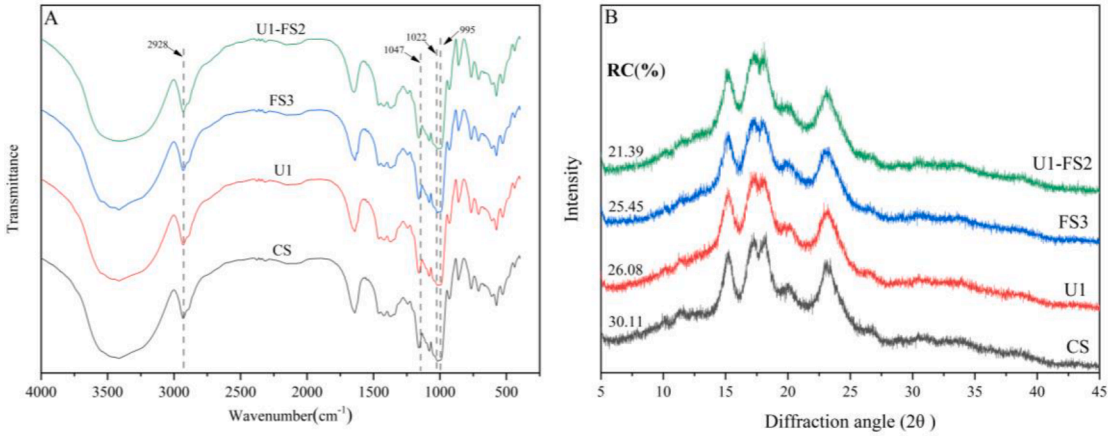

Fig. 6. The short-range and long-range ordered structures of starches with different treatments. The FT-IR characteristics of starches with different treatments (A). The X-ray diffraction patterns of starches with different treatments (B).

ultrasonic and freeze–thaw treatment produced a larger and denser starch structure, and reduced contact with oil. Furthermore, the order and thermal stability of starch were improved, and the oil absorption capacity of starch during frying was inhibited. The results of this study provide a basis for the production of corn starch with low oil absorption by physical modification, which might help to develop healthier fried starch foods with lower oil contents.

Ethical guidelines

Ethics approval was not required for this research.

CRediT authorship contribution statement

Shiyu Zhang: Conceptualization, Methodology, Writing – original draft. **Qi Li:** Data curation, Investigation, Formal analysis. **Yang Zhao:** Investigation, Software, Validation. **Zhixin Qin:** Investigation, Software, Validation. **Mingzhu Zheng:** Conceptualization, Writing – review & editing, Supervision, Funding acquisition. **Huimin Liu:** Conceptualization, Writing – review & editing, Formal analysis. **Jingsheng Liu:** Supervision, Project administration, Funding acquisition.

Declaration of Competing Interest

The authors declare that they have no known competing financial interests or personal relationships that could have appeared to influence the work reported in this paper.

Acknowledgments

This study was supported by the National Special Program for Leading Talents in Grain Industry of China (LL2018201).

References

Aminlari, M., Ramezani, R., & Khalili, M. H. (2016). Production of Protein-Coated Low-Fat Potato Chips. *Food Science and Technology International, 11*(3), 177–181.

Bonto, A. P., Tiozon, R. N., Sreenivasulu, N., & Camacho, D. H. (2021). Impact of ultrasonic treatment on rice starch and grain functional properties: A review. *Ultrasonics Sonochemistry, 71*, Article 105383.

Chanvrier, H., Uthayakumaran, S., Appelqvist, I. A. M., Gidley, M. J., Gilbert, E. P., & López-Rubio, A. (2007). Influence of Storage Conditions on the Structure, Thermal Behavior, and Formation of Enzyme-Resistant Starch in Extruded Starches. *Journal of Agricultural and Food Chemistry, 55*(24), 9883–9890.

Chen, L., McClements, D. J., Yang, T. Y., Ma, Y., Ren, F., Tian, Y. Q., et al. (2021). Effect of annealing and heat-moisture pretreatments on the oil absorption of normal maize starch during frying. *Food Chemistry, 353*, Article 129468.

Chen, L., Tian, Y. Q., Bai, Y. X., Wang, J. P., Jiao, A. Q., & Jin, Z. Y. (2018). Effect of frying on the pasting and rheological properties of normal maize starch. *Food Hydrocolloids, 77*, 85–95.

Chen, L., Tian, Y. Q., Sun, B. H., Cai, C. X., Ma, R. G., & Jin, Z. Y. (2018). Measurement and characterization of external oil in the fried waxy maize starch granules using ATR-FTIR and XRD. *Food Chemistry, 242*, 131–138.

Ching, L. W., Zulkipli, N. A. M., Muhamad, I. I., Marsin, A. M., Khair, Z., & Anis, S. N. S. (2021). Dietary management for healthier batter formulations. *Trends in Food Science & Technology, 113*, 411–422.

Debnath, S., Bhat, K. K., & Rastogi, N. K. (2003). Effect of pre-drying on kinetics of moisture loss and oil uptake during deep fat frying of chickpea flour-based snack food. *LWT - Food Science and Technology, 36*(1), 91–98.

Dehghannya, J., Naghavi, E. A., & Ghanbarzadeh, B. (2015). Frying of Potato Strips Pretreated by Ultrasound-Assisted Air-Drying. *Journal of Food Processing and Preservation, 40*, 583–592.

Diop, C. I. K., Li, H. L., Xie, B. J., & Shi, J. (2011). Impact of the catalytic activity of iodine on the granule morphology, crystalline structure, thermal properties and water solubility of acetylated corn (Zea mays) starch synthesized under microwave assistance. *Industrial Crops and Products, 33*(2), 302–309.

Fauster, T., Schlossnikl, D., Rath, F., Ostermeier, R., Teufel, F., Toepfl, S., et al. (2018). Impact of pulsed electric field (PEF) pretreatment on process performance of industrial French fries production. *Journal of Food Engineering, 235*, 16–22.

Guo, L., Yuan, Y. H., Li, J. H., Tan, C. P., Janaswamy, S., Lu, L., et al. (2021). Comparison of functional properties of porous starches produced with different enzyme combinations. *International Journal of Biological Macromolecules, 174*, 110–119.

Han, J. A., Lee, M. J., & Lim, S. T. (2007). Utilization of oxidized and cross-linked corn starches in wheat flour batter. *Cereal Chemistry, 84*(6), 582–586.

Hu, A. J., Lu, J., Zheng, J., Sun, J. Y., Yang, L., Zhang, X. Q., et al. (2013). Ultrasonically aided enzymatical effects on the properties and structure of mung bean starch. *Innovative Food Science & Emerging Technologies, 20*, 146–151.

Hua, X., Wang, K., Yang, R. J., Kang, J. Q., & Yang, H. (2015). Edible coatings from sunflower head pectin to reduce lipid uptake in fried potato chips. *LWT - Food Science and Technology, 62*(2), 1220–1225.

Jambrak, A. R., Herceg, Z., Šubarić, D., Babić, J., Brnčić, M., Brnčić, S. R., et al. (2010). Ultrasound effect on physical properties of corn starch. *Carbohydrate Polymers, 79*(1), 91–100.

Jeroen, J. G., Soest, V., Tournois, H., Wit, D. D., & Vliegenthart, J. F. G. (1995). Short-range structure in (partially) crystalline potato starch determined with attenuated total reflectance Fourier-transform IR spectroscopy. *Carbohydrate Research, 279*, 201–214.

Liu, Y., Gao, J. M., Wu, H., Gou, M., Jing, L. Z., Zhao, K., Zhang, B., Zhang, G. Q., & Li, W. H. (2019). Molecular, crystal and physicochemical properties of granular waxy corn starch after repeated freeze-thaw cycles at different freezing temperatures. *International Journal of Biological Macromolecules, 133*, 346–353.

Liu, Z. Y., Wang, C., Liao, X. J., & Shen, Q. (2020). Measurement and comparison of multi-scale structure in heat and pressure treated corn starch granule under the same degree of gelatinization. *Food Hydrocolloids, 108*, Article 106081.

Luo, Y., Han, X. Y., Shen, M. Y., Yang, J., Ren, Y. M., & Xie, J. H. (2021). Mesona chinensis polysaccharide on the thermal, structural and digestibility properties of waxy and normal maize starches. *Food Hydrocolloids, 112*. p. 106317.

Qiao, D. L., Xie, F. W., Zhang, B. J., Zou, W., Zhao, S. M., Niu, M., et al. (2017). A further understanding of the multi-scale supramolecular structure and digestion rate of waxy starch. *Food Hydrocolloids, 65*, 24–34.

Santha, N., Sudha, K. G., Vijayakumari, K. P., Nayar, V. U., & Moorthy, S. N. (1990). Raman and infrared spectra of starch samples of sweet potato and cassava. *Journal of Chemical Sciences, 102*(2), 705–712.

Sevenou, O., Hill, S. E., Farhat, I. A., & Mitchell, J. R. (2002). Organisation of the external region of the starch granule as determined by infrared spectroscopy. *International Journal of Biological Macromolecules, 31*(1–3), 79–85.

Šimková, D., Lachman, J., Hamouz, K., & Vokál, B. (2013). Effect of cultivar, location and year on total starch, amylose, phosphorus content and starch grain size of high starch potato cultivars for food and industrial processing. *Food Chemistry, 141*(4), 3872–3880.

Sujka, M. (2017). Ultrasonic modification of starch - Impact on granules porosity. *Ultrasonics Sonochemistry, 37*, 424–429.

Tao, H., Wang, P., Wu, F. F., Jin, Z. Y., & Xu, X. M. (2016). Particle size distribution of wheat starch granules in relation to baking properties of frozen dough. *Carbohydrate Polymers, 137*, 147–153.

Tao, H., Yan, J., Hao, J., Tian, Y., Jin, Z., & Xu, X. (2015). Effect of multiple freezing/thawing cycles on the structural and functional properties of waxy rice starch. *PLoS One, 10*(5). p. e0127138.

Timm, N. D. S., Ramos, A. H., Ferreira, C. D., Biduski, B., Eicholz, E. D., & Oliveira, M. (2020). Effects of drying temperature and genotype on morphology and technological, thermal, and pasting properties of corn starch. *International Journal of Biological Macromolecules, 165*(PTA), 354–364.

Vadgama, B., & Harris, D. K. (2007). Measurements of the contact angle between R134a and both aluminum and copper surfaces. *Experimental Thermal and Fluid Science, 31*(8), 979–984.

Vamadevan, V., & Bertoft, E. (2015). Structure-function relationships of starch components. *Starch-Stärke, 67*(1–2), 55–68.

Wang, H., Xu, K., Ma, Y., Liang, Y., Zhang, H., & Chen, L. (2020). Impact of ultrasonication on the aggregation structure and physicochemical characteristics of sweet potato starch. *Ultrasonics Sonochemistry, 63*, Article 104868.

Yang, D., Wu, G. C., Li, P. Y., Qi, X. G., Zhang, H., Wang, X. G., et al. (2020). The effect of fatty acid composition on the oil absorption behavior and surface morphology of fried potato sticks via LF-NMR, MRI, and SEM. *Food Chemistry X, 7*, Article 100095.

Ye, J. P., Liu, C. G., Luo, S. J., Hu, X. T., & McClements, D. J. (2018). Modification of the digestibility of extruded rice starch by enzyme treatment (beta-amylolysis): An in vitro study. *Food Research International, 111*, 590–596.

Yousif, E. I., Gadallah, M. G. E., & Sorour, A. M. (2012). Physico-chemical and rheological properties of modified corn starches and its effect on noodle quality. *Annals of Agricultural Sciences, 57*(1), 19–27.

Zeng, H., Chen, J. W., Zhai, J. L., Wang, H. B., Xia, W. S., & Xiong, Y. L. (2018). Reduction of the fat content of battered and breaded fish balls during deep-fat frying using fermented bamboo shoot dietary fiber. *LWT, 73*, 425–431.

Zhang, B., Xiao, Y. W., Wu, X. N., Luo, F. J., Lin, Q. L., & Ding, Y. B. (2021). Changes in structural, digestive, and rheological properties of corn, potato, and pea starches as influenced by different ultrasonic treatments. *International Journal of Biological Macromolecules, 185*, 206–218.

Zhang, J., Yu, P. B., Fan, L. P., & Sun, Y. (2021). Effects of ultrasound treatment on the starch properties and oil absorption of potato chips. *Ultrason Sonochemistry, 70*, Article 105347.

Zhao, H., Law, K. Y., & Sambhy, V. (2011). Fabrication, surface properties, and origin of superoleophobicity for a model textured surface. *Langmuir the ACS Journal of Surfaces & Colloids, 27*(10), 5927–5935.

Zhu, C. Y., Li, G. S., Xing, Y. W., & Gui, X. H. (2021). Adhesion forces for water/oil droplet and bubble on coking coal surfaces with different roughness. *International Journal of Mining Science and Technology, 31*(4), 681–687.

Zhu, J., Li, L., Chen, L., & Li, X. X. (2012). Study on supramolecular structural changes of ultrasonic treated potato starch granules. *Food Hydrocolloids, 29*(1), 116–122.